INSTITUTE OF PHYSICS PUBLISHING JOURNAL OF PHYSICS: CONDENSED MATTER

J. Phys.: Condens. Matter **19** (2007) 036214 (12pp) doi:10.1088/0953-8984/19/3/036214

Mixed $PbFBr_{1-x}I_x$ crystals: structural and spectroscopic investigations

H Hagemann[1,5], A Rief[2], F Kubel[2], J L M van Mechelen[3], F Tran[4] and P Blaha[4]

[1] Department of Physical Chemistry, University of Geneva, 30, quai Ernest-Ansermet, CH-1211 Geneva 4, Switzerland
[2] Institute of Chemical Technologies and Analytics, Vienna University of Technology, Getreidemarkt 9/164-SC, A-1060 Vienna, Austria
[3] Department of Condensed Matter Physics, University of Geneva, 24, quai Ernest-Ansermet, CH-1211 Geneva 4, Switzerland
[4] Institute of Materials Chemistry, Vienna University of Technology, Getreidemarkt 9/165-TC, A-1060 Vienna, Austria

E-mail: hans-rudolf.hagemann@chiphy.unige.ch

Received 29 September 2006
Published 5 January 2007
Online at stacks.iop.org/JPhysCM/19/036214

Abstract

Mixed single $PbFBr_{1-x}I_x$ crystals have been prepared. X-ray powder diffraction structure determinations show that all samples crystallize with the matlockite structure. However, the single crystal structure of $PbFBr_{0.5}I_{0.5}$ involves not only fractional occupation of one site corresponding to the stoichiometry, but also split positions of the Pb^{2+} ion. Raman spectra reveal the presence of new additional bands with respect to PbFBr and PbFI. DFT calculations of lattice vibrations for PbFI show good agreement with experimental spectra. The calculated phonon dispersion curve suggests that for the mixed crystals the centre of inversion is conserved locally. These combined results suggest the presence of domains with ordered F–Pb–Br–Br–Pb–F and F–Pb–I–I–Pb–F layers in the mixed crystals. Calculations on $PbFBr_{0.5}I_{0.5}$ show that this suggested structure is more stable than the structure consisting of the F–Pb–Br–I–Pb–F arrangement.

(Some figures in this article are in colour only in the electronic version)

1. Introduction

Crystals of the matlockite (PbFCl) family have been the subject of numerous investigations with respect to a variety of potential applications such as room temperature hole burning [1],

[5] Author to whom any correspondence should be addressed.

radiation detection [2] and pressure sensors [3]. More recently, the compound PbFCl has been studied as scintillator material [4].

In the course of our investigations on mixed PbFCl-type crystals, we have studied crystals of $BaFBr_{1-x}I_x$ [5]. In contrast to other mixed crystals of this family, e.g. $SrFBr_{1-x}Cl_x$ [6], the crystal structure of $BaFBr_{1-x}I_x$ can only be satisfactorily modelled by introducing a split position of the Ba ion in addition to the fractional occupation of the heavy halogen site. In this investigation, it was shown that there is a 'local' lowering of crystal symmetry (ferrielectric domains) which is seen by vibrational spectroscopy and ESR on Eu-doped samples, but not by single crystal x-ray diffraction.

In this work we address the crystal structure of the analogous lead compounds $PbFBr_{1-x}I_x$. In addition to the crystallographic study, the Raman spectra of the starting compounds PbFI and PbFBr are compared with those of the mixed crystals. The experimental data are further compared with theoretical calculations of lattice vibrations in PbFI and terahertz transmission spectra.

2. Experimental details

2.1. Sample preparation

Powder samples and single crystals were prepared from stoichiometric amounts of Pro Analytical PbF_2, $PbBr_2$ and PbI_2 (Merck) by hydrothermal synthesis. The samples were annealed with demineralized water in Teflon crucibles placed in steel autoclaves at 250 °C for up to 87 days. Polycrystalline material was obtained after 20 days, single crystals suitable for measurements with a size of around 100 μm after 60 days. Platelike single crystals were found; the crystals were used for single crystal diffraction after optical examination under a high precision optical microscope. Powders of different stoichiometries with a nominal Br/I ratio of 25/75, 50/50 and 75/25 were prepared and analysed by powder diffraction methods. Samples for single crystal growth were prepared using a 50/50 Br/I ratio.

2.2. Powder diffraction

X-ray measurements on polycrystalline samples were made on a Philips X-PERT Bragg–Brentano diffractometer. Rietveld refinement using the fundamental parameter approach with TOPAS 2.0[6] allowed us to calculate the lattice parameters and the phase composition. As matlockite tends to show texture effects due to its platelike habitus, a calculation of texture effects along [001] was included in the refinement.

2.3. Single crystal diffraction

Single crystal measurements were made on a Nonius CAD4 diffractometer. Collected intensities were refined with the program package XTAL 3.2. [7]. Experimental conditions for the single crystal structure determination are summarized in table 1. Atomic positions and isotropic (anisotropic) and atomic displacement factors are listed in table 2.

2.4. Raman measurements

For observations at very low Raman shifts, measurements were made on powdered samples using either a Spex 1403 or 1404 double monochromator with excitation wavelengths of 488 and 568 nm. This last one provided the best S/N data for the yellow powdered samples.

[6] Topas Software for Rietveld Refinement by Bruker AXS.

Table 1. Single crystal diffraction data of $PbFBr_{0.5}I_{0.5}$ at 300 K.

Formula	$PbFBr_{0.5}I_{0.5}$
Space group/system	Tetragonal $P4/nmm$ (129)
$a = b$ (Å)	4.2087(6)
c (Å)	8.1491(22)
V (Å^3)	144.35(5)
Calc. density (g cm^{-1})	7.583
Z	1
Diffractometer type	Nonius CAD 4
Wavelength (Å)	Mo Kα 0.710 73
Monochromator	Graphite
Method	ω-scan
Temperature (K)	293
Crystal size in mm $\times 100$	$1.2 \times 0.9 \times 0.3$
θ range (deg.)	5–30
n_{ref} measured	1046
$h_{\mathrm{max}}/h_{\mathrm{min}}$	$5/-5$
$k_{\mathrm{max}}/k_{\mathrm{min}}$	$5/-5$
$l_{\mathrm{max}}/l_{\mathrm{min}}$	$11/-8$
n_{ref} independent	155
Program used	XTAL 3.2 [7]
n_{ref} with $I > 3\sigma(I)$	112
R_{int} (%)	5.7
R (R_w)	5.4 (5.4)
Goodness of fit	2.46
Number of parameters	10
$e^-_{\mathrm{Min/max}}$	$-2.42/5.41$
ICSD number	417 019

Table 2. Atomic positions and isotropic (anisotropic) and atomic displacement factors of $PbFBr_{0.5}I_{0.5}$.

	x/a	y/b	z/c	$U(eq)$	PP (fixed)
Pb(1)	1/4	1/4	0.141 7(2)	0.0240(3)	0.5
Pb(2)	1/4	1/4	0.215 3(2)	0.0295(3)	0.5
F(1)	3/4	1/4	0.037 8(13)	0.030(3)	0.5
Br(1)	1/4	1/4	0.659 85(17)[a]	0.0424(4)[a]	0.5
I(1)	1/4	1/4	0.659 85(17)[a]	0.0424(4)[a]	0.5
	U_{11} (F: U(iso))		U_{22}	U_{33}	
Pb(1)	0.194(3)[a]		U_{11}	0.0628(15)[a]	
Pb(2)	0.194(3)[a]		U_{11}	0.0628(15)[a]	
F (isotropic)	0.030(3)		—	—	
Br(1)	0.0206(4)[a]		U_{11}	0.0853(11)[a]	
I(1)	0.0206(4)[a]		U_{11}	0.0853(11)[a]	

[a] Constrained value.

Additional experiments were performed at room temperature using a Labram Raman microscope with an excitation wavelength of 532 nm in the backscattering geometry. As the crystals grow as platelets perpendicular to the c-axis, one observes in this geometry combinations of (a, a), (b, b) and (a, b) polarizations, allowing one thus to observe the weak single B_{1g} mode around 210 cm^{-1} (polarization (a, b)).

2.5. Terahertz transmission

Terahertz transmission experiments were performed between 1.5 and 90 cm^{-1} with a resolution of 1 cm^{-1} at 300 K on powdered samples dispersed in polyethylene pellets using a Teraview TPI Spectra 1000 time-domain spectrometer.

2.6. Theoretical calculations

The calculations on the PbFI and $PbFBr_{0.5}I_{0.5}$ compounds were done with the WIEN2k code [8] which is based on the full-potential (linearized) augmented plane-wave plus local orbitals (FP-(L)APW + lo) method to solve the Kohn–Sham [9] equations of density functional theory (DFT) [10] in solids. The PBE [11] functional, of the generalized gradient approximation (GGA) form, was chosen for the exchange–correlation energy. For PbFI, the geometry optimization and phonon calculations at the Γ point were done with a 13 × 13 × 5 special point grid for the Brillouin zone integrations and $R_{MT}^{min} K_{max} = 8$ was used for the expansion of the basis set. The phonons were calculated using a real space force constant fitting based on forces calculated for symmetry adapted atomic displacements [12]. The LO/TO splitting of the infrared-active mode was not included. A 2 × 2 × 2-supercell was used for the calculation of the phonons of PbFI in the full Brillouin zone, and reduced parameters were used for this calculation ($5 \times 5 \times 2$ for the special point grid and $R_{MT}^{min} K_{max} = 7$). For $PbFBr_{0.5}I_{0.5}$, a $9 \times 9 \times 2$ special point grid for the Brillouin zone integrations was used. The sphere radii were chosen as 2.32 au for F and Pb atoms and 2.5 au for Br and I atoms. Scalar relativistic effects were considered in the calculations, but spin–orbit coupling was not included, as the calculation of the forces with spin–orbit coupling (needed for the optimization of the internal parameters) is not implemented in the code.

3. Results and discussion

3.1. Crystal structure

The powder diffraction data show that $PbFBr_{1-x}I_x$ crystallizes in the matlockite (PbFCl) structure. In a first approach, it was assumed that the bromide and iodide ions occupy the same site (Wyckoff site 2c) in a statistic arrangement. The powder diffraction data of the mixed samples indicate a rather homogeneous composition, i.e. there is no significant distribution of lattice parameters. The lattice constants and bond distances show a linear behaviour over different Br/I ratios, in agreement with Vegard's law. Figure 1 shows the unit cell volume and the Pb–Br/I bond distances as a function of iodine concentration, including the single crystal data reported for PbFBr [13] and PbFI [14]. This behaviour was expected from our previous studies of mixed (Sr, Ba)F(Cl, Br) crystals [6, 15]. In PbFI or PbFBr, a simple stacking order along the *c*-axis of –X–Pb–F–Pb–X–X–Pb–F–Pb–X– (with X = Br, I) is observed; in the mixed Br/I samples the layer arrangement is more complex, as will be shown below.

Experimentally, it can be seen from figure 1 that the sample with a nominal iodide content of 25% may tend to a higher bromide content (confirmed also by Raman measurements). The deviation from the linear behaviour suggests a real Br:I ratio content of approximately 85%:15%. X-ray refinement on this sample showed a iodide-rich secondary-phase PbFI (1.8(2) wt%) confirming this trend.

In the first structure refinement from the single crystal diffraction data based on the matlockite structure, the lead ion had an inconsiderably high anisotropy in vibrational parameters, which suggested a split position of the lead ion ($U_{11} = 0.0193(3)$, $U_{33} = 0.1820(12)$ $Å^2$). Refining the structure with a split lead position along the *c*-axis (Pb(1) $z/c = 0.1417(2)$ and Pb(2) $z/c = 0.2154(2)$) gives reasonable anisotropy of $U_{33}(Pb) = 0.063(2)$

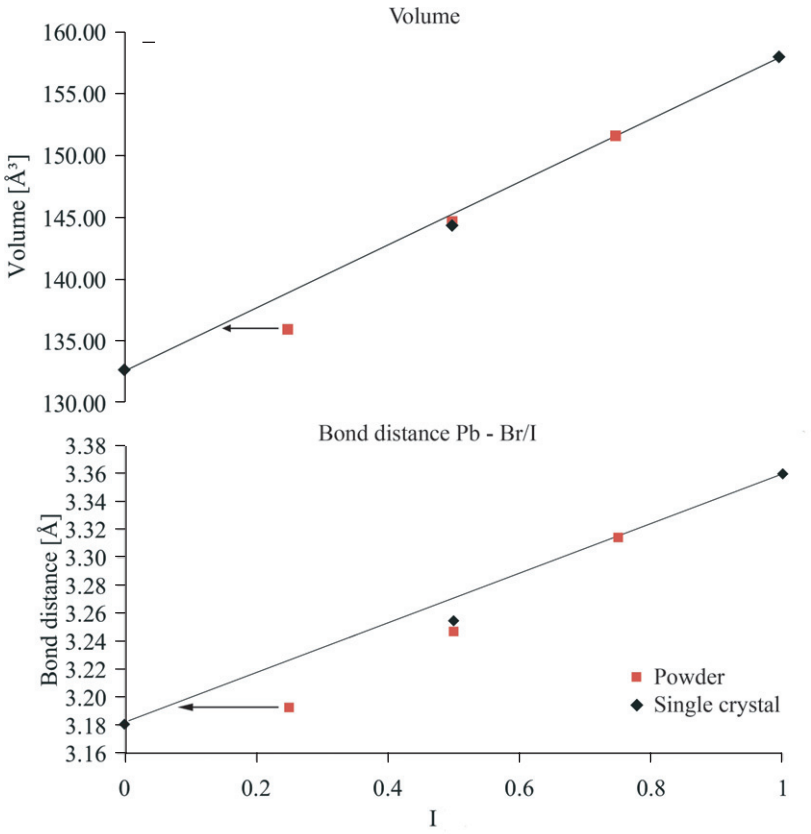

Figure 1. Unit cell volume and metal–heavy halide bond distance drawn versus iodide content. The data for PbFBr and PbFI are taken from [13, 14].

and a better R value. The high anisotropy of the fluoride ion along the c-axis agrees well with this model: the average value of the Pb–F distance (2.56 Å) is in the same range as the corresponding value in PbFBr and PbFI [13, 14]. The Pb–Br/I distances vary between 3.1449(8) and 3.3870(11) Å in the lead coordination sphere (figure 3). In the final refinement, the fluoride was split in two positions with nominal occupation of 50%. The corresponding structural parameters are collected in table 2.

With this model, the statistical occupation of the bromide/iodide position within one layer appears unlikely, as it would lead to significant strains in the structure.

Figure 2 shows schematically three different possible substitution models. At the top, a mixed order statistically occupying the same site is assumed. This has been observed for instance in $BaFCl_{0.57}Br_{0.43}$ [15]. A stacking order along the c-axis with halogen layers filled by only one halide ion (either Br or I) can be arranged either in double layers or single layers (see figure 2). In these latter models, the layers are filled by one sort of ion but arranged statistically along the c-axis (no hint of super-structure reflexes could be found in the powder pattern or single crystal measurements). If the structure were arranged in a fixed order (e.g. · · ·–I–I–· · ·–Br–Br–· · ·–I–I–· · ·) additional signals should be seen in the diffraction patterns.

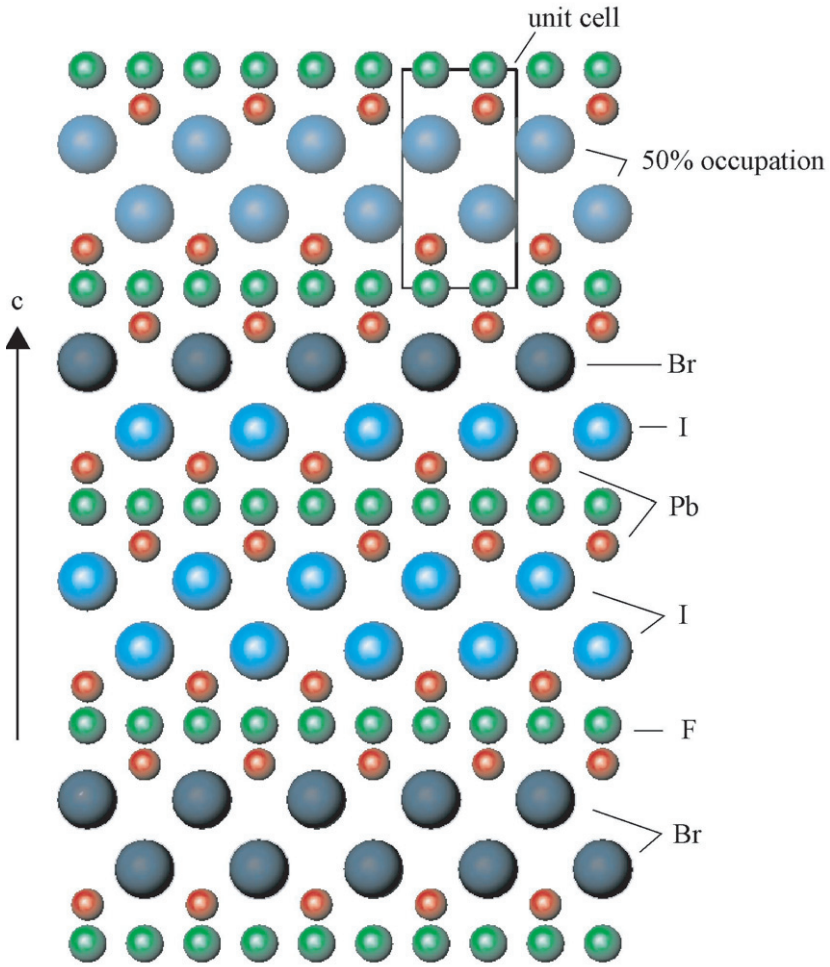

Figure 2. Schematic drawing of possible arrangements of bromide and iodide layers in the mixed crystal in the case of 50% substitution. The upper part shows a statistical distribution, the two lower parts different models with uniformly occupied layers of one heavy halogen (either bromide or iodide).

The lead ion in the matlockite shows 8 + 1- (PbFBr) and 8 + 2- (PbFI) fold coordination to the neighbouring halides (see figure 3) with a weak coordination to the next layers of halide ions.

3.2. Raman spectra

Group theory predicts for PbFBr and PbFI six Raman active modes (three E_g, two A_{1g} and B_{1g}). The symmetry coordinate analysis shows that the single B_{1g} mode corresponds to a motion involving only fluoride ions.

The Raman spectra of PbFBr and PbFI as well as those of samples with nominal Br:I ratios of 25:75, 50:50 and 75:25 are shown in figure 4. The corresponding band positions are collected in table 3.

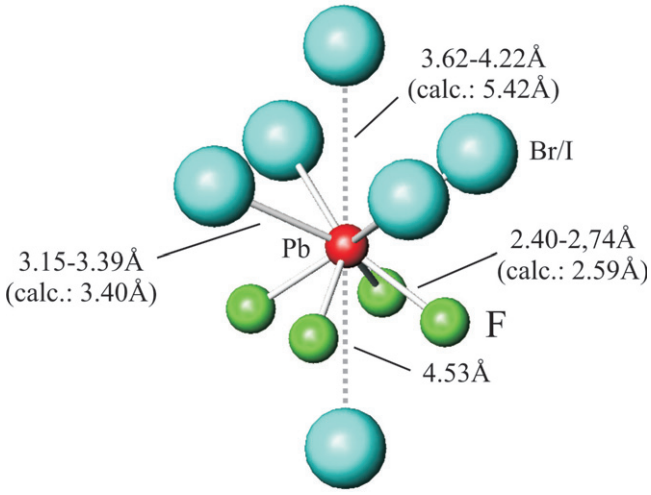

Figure 3. Lead coordination sphere. Bond distances between Pb and I vary depending on the substitution ratio, Pb–F distances are nearly the same for all ratios. Values given are Br^-/I^-–Pb^{2+} distance in mixed crystals assuming a split position for lead. Values calculated with the WIEN2k code for PbFI are in parentheses.

Table 3. Raman data for matlockite crystals at room temperature. Literature data for BaFX [23] are included for comparison (w = weak, br = broad, sh = shoulder). Peak positions are given within $\pm 0.5\ cm^{-1}$.

Compound	E_g		E_g	A_{1g}	A_{1g}	B_{1g}	E_g
BaFCl [23]	82		143	132	165	216	251
BaFBr [23]	76		109	103	123	211	238
BaFI [23]	67		111	78	102	203	219
PbFCl [16]	43.5		134	105.5	164.5	226.5	241
PbFBr [16]	39		94.5	~89	116.5	224.5	
(This work)	39		93.5	~87sh	116	221	
$PbFBr_{0.75}I_{0.25}$	37.7	65w, br	~87sh	91.2	114	219.5	
$PbFBr_{0.5}I_{0.5}$	30 + 37.2	60	80	~85sh	113 + 104sh	216.5	
$PbFBr_{0.25}I_{0.75}$	36.1 + 27.5		67.5	~77sh	106.5	211.5	
PbFI [16]	36		60	67	102		
(This work)	36		61.4	67	105.5	206	

All spectra show a relatively strong band close to 38 cm^{-1}, which has been assigned by Rulmont [16] to the lowest frequency E_g mode. This assignment is further confirmed by the periodic DFT calculation (see below).

Our data for PbFBr and PbFI are in agreement with those reported by Rulmont [16], and in the case of PbFI the previously unobserved B_{1g} mode could be clearly identified at 206 cm^{-1}. In the case of PbFBr, we do observe a weak and broad band around 180 cm^{-1}, the origin of which is not clear.

It is interesting to note the strong decrease in relative intensity of the B_{1g} mode (around 210 cm^{-1}) when going from the bromide to the iodide. As this band should be the least affected by the solid solution (being a purely fluoride motion), one could expect that the frequency of this bands varies linearly with composition. This behaviour has been observed in the similar

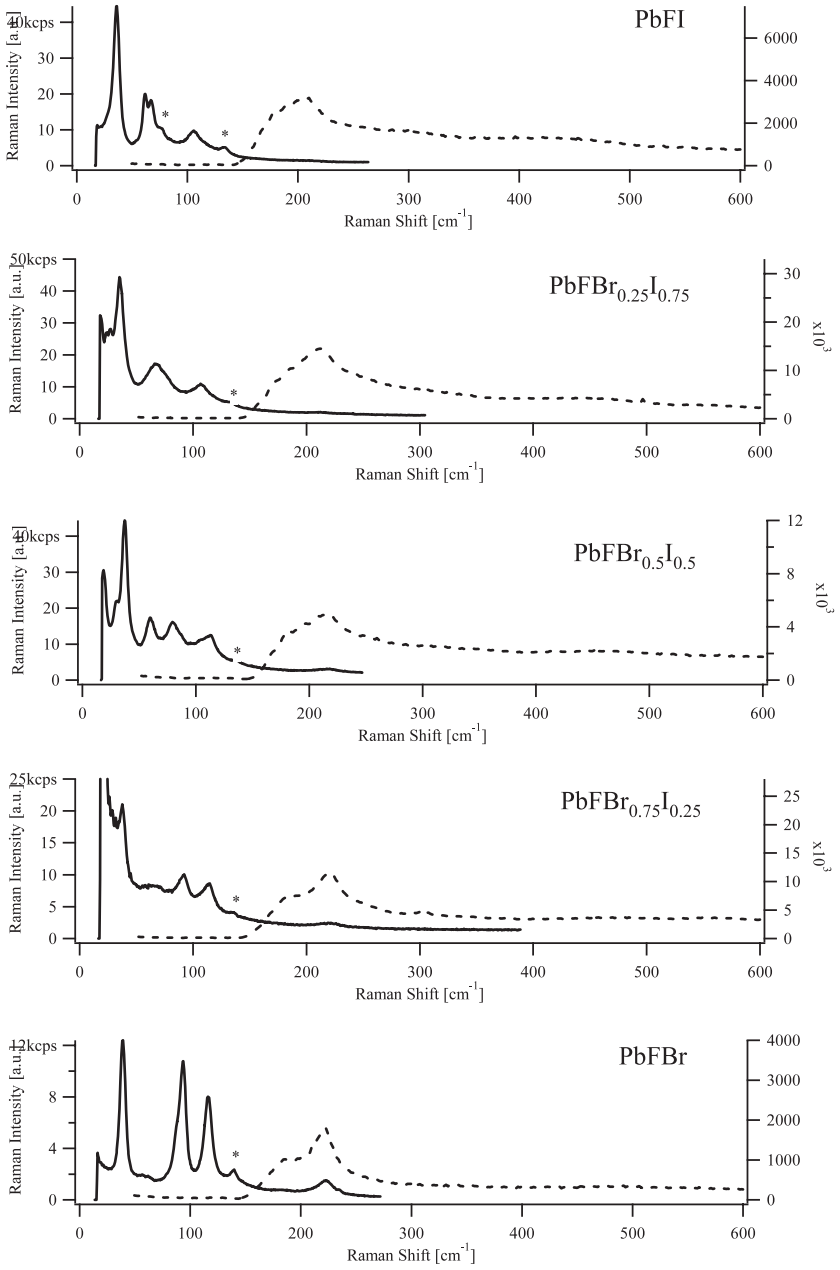

Figure 4. Room temperature Raman spectra of powdered PbFX (568 nm excitation, full line) and partially polarized micro-Raman spectra of individual crystal platelets (532 nm excitation, dotted line) to reveal the B_{1g} mode for all samples. Bands below 180 cm^{-1} could not be observed with the micro-Raman experiment. Weak bands labelled $*$ are from impurities in the powder samples.

systems SrFCl–SrFBr [17], BaFCl–BaFBr and SrFCl–BaFCl [18]. The data collected in table 3 suggest that the samples with nominal Br:I compositions 75:25 and 50:50 appear to be richer in bromide with respect to their nominal compositions. This trend is in agreement with the x-ray diffraction data shown above.

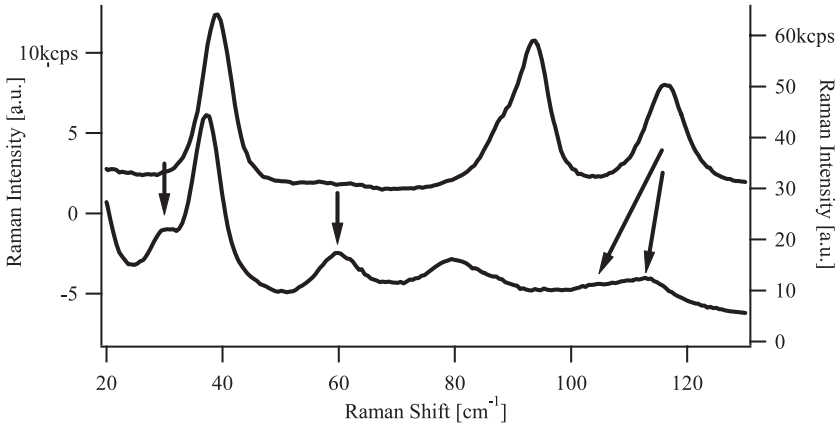

Figure 5. Comparison of low frequency Raman spectra of PbFBr (upper trace) and $PbFBr_{0.5}I_{0.5}$ (nominal composition). The arrows show the splitting of the single band at 116 cm^{-1} and the new band at 60 cm^{-1} as well as the band at 30 cm^{-1} discussed in the text.

Table 4. Calculated and experimental [14] lattice (a and c, in Å) and internal (z_I/c and z_{Pb}/c) parameters of the PbFI compound. The values of z_I/c and z_{Pb}/c in parenthesis were determined at the experimental lattice parameters.

	a	c	c/a	z_I/c	z_{Pb}/c
Calc.	4.227	10.02	2.371	0.690 (0.659)	0.149 (0.167)
Expt	4.2374	8.800	2.077	0.663	0.164

Figure 5 amplifies the low frequency Raman spectra of PbFBr and $PbFBr_{0.5}I_{0.5}$. In this spectral region, four Raman active bands are expected for PbFBr. In the mixed compound, however, the highest and lowest bands appear to split into two components, as shown by the arrows for one component, and a new feature emerges at 60 cm^{-1}.

This behaviour is in contrast with the regular evolution of the Raman spectra in the solid solutions $SrFCl_xBr_{1-x}$ [17], where no breakdown of selection rules was observed.

3.3. Theoretical calculations

In order to obtain more insight into the origin of these spectral splittings, we have calculated the lattice vibrations of PbFI using DFT methods. First, a full geometry optimization of the PbFI compound was done. To this end, a scan of the potential energy surface was made by varying the lattice parameters a and c, and for different values of a and c the internal parameters z_I/c and z_{Pb}/c were also optimized. The results of this procedure are shown in table 4 along with the experimental results [14]. The results show that a very good agreement is found for the lattice parameter a, which is underestimated by only 0.01 Å, while a large overestimation of about 1.2 Å is found for c (8.80 Å for the experimental value versus 10.02 Å for the calculated value). This overestimation of c is not surprising, since the GGA PBE exchange–correlation functional is known to have the trend to overestimate the separation between weakly interacting layers (see, e.g., [19]). As evident from figure 3, the large c is a direct consequence of the largely overestimated I–I distance. Note that in [20] a lattice constant $c = 9.152$ Å was found for PbFI with the same functional (PBE). An explanation of their different results could be that they determined the equilibrium volume by keeping the internal parameters fixed, or

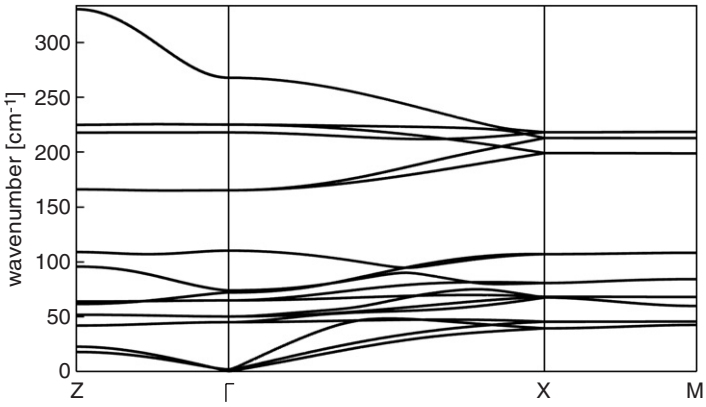

Figure 6. Calculated phonon dispersion curve for PbFI.

Table 5. Calculated and experimental Raman (R) and infrared (I) vibrational frequencies (in cm^{-1}) of PbFI. The second column indicates which atoms (and in which directions) are involved in the vibrational mode (atoms whose contributions are small are not shown).

Symmetry	Atoms	Calc.[a]	Calc.[b]	Expt
$E_g(R)$	$Pb_1(x, y)$, $Pb_2(-x, -y)$, $I_1(-x, -y)$, $I_2(x, y)$	36	41	36
$E_u(I)$	$Pb_1(-x, -y)$, $Pb_2(-x, -y)$, $F_1(x, y)$, $F_2(x, y)$, $I_1(x, y)$, $I_2(x, y)$	35	47	50, 62 [16]
$E_g(R)$	$Pb_1(-x, -y)$, $Pb_2(x, y)$, $F_1(x, -y)$, $F_2(-x, y)$, $I_1(-x, -y)$, $I_2(x, y)$	40	64	61
$A_{2u}(I)$	$Pb_1(-z)$, $Pb_2(-z)$, $I_1(z)$, $I_2(z)$	79	71	
$A_{1g}(R)$	$Pb_1(z)$, $Pb_2(-z)$, $I_1(-z)$, $I_2(z)$	61	73	67
$A_{1g}(R)$	$Pb_1(z)$, $Pb_2(-z)$, $I_1(z)$, $I_2(-z)$	108	109	105
$E_u(I)$	$F_1(x, y)$, $F_2(x, y)$	141	150	142, 154 [16]
$B_{1g}(R)$	$F_1(-z)$, $F_2(z)$	194	207	206
$E_g(R)$	$F_1(-x, -y)$, $F_2(x, y)$	212	217	
$A_{2u}(I)$	$F_1(z)$, $F_2(z)$	274	259	318, 332 [16]

[a] Calculated at the theoretical lattice parameters (see table 4).
[b] Calculated at the experimental lattice parameters.

that they used smaller convergence parameters (e.g. $R_{MT}^{min}K_{max} = 7$) for the calculations. It should be mentioned that for the BaFCl compound recent calculations did not result in such a large overestimation for c for any of the tested functionals [21]. The calculated internal parameters z_I/c and z_{Pb}/c also show discrepancies with respect to the experimental values. This disagreement is a direct consequence of the too large theoretical value of c, since, with the experimental lattice constants, the calculated z_I/c and z_{Pb}/c (also shown in table 4) are in very good agreement with the experimental values.

Raman and infrared vibrational frequencies were calculated both at the experimentally and theoretically determined lattice parameters. The results, displayed in table 5, show that overall a fairly good agreement between the theoretical and experimental sets of data is obtained. The eigenvectors confirm that the modes calculated at frequencies above 150 cm^{-1} are mainly fluoride motions, in agreement with the results reported for BaFCl [21]. However, in particular for the theoretical lattice parameters, the lowest E_u and second E_g modes are underestimated by about 20 cm^{-1}. The highest A_{2u} mode is greatly underestimated at both sets of lattice parameters because we neglected the long ranged LO/TO splitting due to effective ionic charges. The strong overestimation of the lattice parameter c is probably at the origin of the less satisfying agreement obtained with the frequencies at the theoretical lattice parameters.

The calculated phonon dispersion curve is shown in figure 6. The lowest frequency zone-centre mode (calculated at 41 cm^{-1}) is Raman active, followed by the IR active mode at

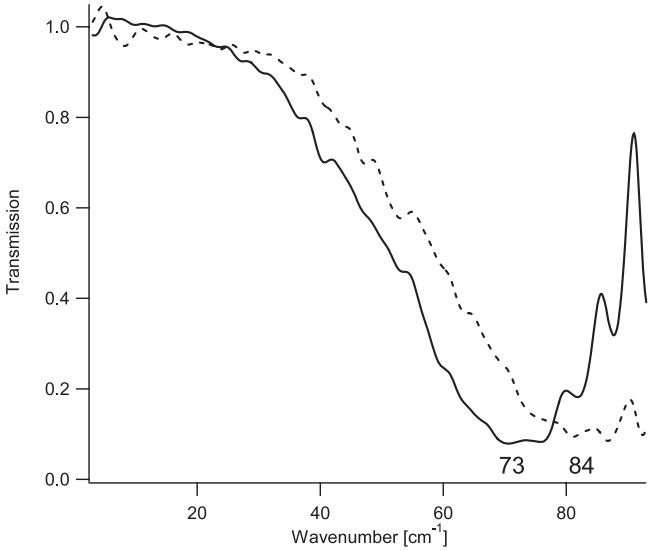

Figure 7. Terahertz transmission spectra of powdered samples dispersed in polyethylene: full line PbFI, dashed line $PbFBr_{0.5}I_{0.5}$. The oscillations which appear above about 80 cm^{-1} are not reproducible and probably related to some artefact due to the fact that above about 80 cm^{-1} the detector response is about five orders of magnitude smaller than around 30 cm^{-1}.

47 cm^{-1} (see table 5). It is important to note that the frequency of this IR active mode always remains larger than the one of the lowest frequency Raman active mode. If some kind of superstructure (on the length scale probed by the Raman experiment) is present, the new zone-centre modes can be evaluated by back-folding the dispersion curve.

3.4. Terahertz transmission

Recent FIR measurements on PbFBr show the presence of IR-active bands which are observed between 56 and 79 cm^{-1} [22], but no additional IR bands are expected at lower frequencies. Figure 7 shows the transmission spectra of PbFI and $PbFBr_{0.5}I_{0.5}$ which show indeed no band below 50 cm^{-1}. For PbFI, we observe a broad band centred at about 73 cm^{-1}, which is somewhat higher than the value of 62 cm^{-1} reported by Rulmont [16]. This band shifts to about 84 cm^{-1} for $PbFBr_{0.5}I_{0.5}$, but it must be noted that in this spectral range the instrument response is much weaker. Rulmont [16] reported a value of 78 cm^{-1} for PbFBr, which gives a spectral shift of $78 - 62 = 16$ cm^{-1} between the bromide and the iodide. The spectral shift between PbFI and $PbFBr_{0.5}I_{0.5}$ seen in figure 7 falls in this range.

These observations, in conjunction with the calculated phonon dispersion curve, indicate that the new band observed at 30 cm^{-1} in the Raman spectrum of $PbFBr_{0.5}I_{0.5}$ cannot be explained by an IR active mode which also becomes Raman active by the suppression of the inversion symmetry. A possible explanation for the presence of this band as well as the other additional features observed is a lowering of the local symmetry (on the length scale probed by Raman spectroscopy) from tetragonal to orthorhombic, resulting in the splitting of the doubly degenerate E_g modes, or alternatively by a local (tetragonal) superstructure along the *c*-axis which preserves the inversion symmetry by forming vertical layers of alternating F–Pb–Br–Br–Pb–F–Pb–I–I–Pb–F sheets (see figure 2). Considering the fact that the lowest energy Raman bands in PbFBr and PbFI are very close (39 and 36 cm^{-1}), a splitting of this E_g band into two

components at 30 and 37 cm^{-1} (as observed for $PbFBr_{0.5}I_{0.5}$) does not appear to be very likely, but cannot be ruled out.

In order to verify the experimental suggestion about a local inversion centre with double layers of Br and I (F–Pb–Br–Br–Pb–F–Pb–I–I–Pb–F), DFT calculations on $PbFBr_{0.5}I_{0.5}$ for two of the structures of figure 2 (the suggested one and F–Pb–Br–I–Pb–F) with a doubled unit cell were done. After relaxation of all atomic positions we found the suggested structure more stable than the other one by 8.6 meV per formula unit, thus supporting the experimental findings.

4. Conclusions

The single crystal x-ray structure of the mixed $PbFBr_{0.5}I_{0.5}$ crystals has been found to present similar anomalies to the corresponding Ba compounds. These anomalies are further manifested by a breakdown of Raman selection rules, which has not been observed in other mixed crystals of the matlockite family such as $SrFCl_{1-x}Br_x$. Fundamentally, these observations appear to be associated with some form of local order within an otherwise normally behaving mixed crystal. The current results suggest the conservation of a local inversion centre (on the length scale of the Raman spectroscopy) leading to double layers of bromide and iodide. Further experiments are necessary to fully characterize the structure of these mixed compounds.

Acknowledgments

This work was supported by the Swiss National Science Foundation and the Austrian Grid (WP A-7).

References

[1] Jaaniso R and Bill H 1991 *Europhys. Lett.* **16** 569
[2] Brixner L H 1987 *Mater. Chem. Phys.* **16** 253
[3] Shen Y R, Gregorian T and Holzapfel W 1991 *High Pressure Res.* **7** 73
[4] Liu B, Shi C S, Chen J M and Shen D Z 2005 *IEEE Trans. Nucl. Sci.* **52** 527
[5] Rey J, Bill H, Hagemann H and Kubel F 2005 *Phys. Rev.* B **72** 184107
[6] Hagemann H, Kubel F and Bill H 1993 *Mater. Res. Bull.* **28** 353
[7] Hall S R, Flack H D and Steward J M (ed) 1992 *XTAL 3.2 Reference Manual* Universities of Western Australia, Geneva and Maryland/Lamb, Perth
[8] Blaha P, Schwarz K, Madsen G K H, Kvasnicka D and Luitz J 2001 *WIEN2k, An augmented Plane Wave + Local Orbitals Program for Calculating Crystal Properties (Vienna University of Technology, Austria)* ed K Schwarz ISBN 3-9501031-1-2
[9] Kohn W and Sham L J 1965 *Phys. Rev.* **140** A1133
[10] Hohenberg P and Kohn W 1964 *Phys. Rev.* **136** B864
[11] Perdew J P, Burke K and Ernzerhof M 1996 *Phys. Rev. Lett.* **77** 3865
Perdew J P, Burke K and Ernzerhof M 1997 *Phys. Rev. Lett.* **78** 1396
[12] Parlinski K 2002 Software PHONON, Cracow
[13] Nieuwenkamp W and Bijvoet J M 1932 *Z. Kristallogr.* **81** 157
[14] Weil M and Kubel F 2001 *Acta Crystallogr.* E **57** i80
[15] Hagemann H, Tissot P, Lovy D, Kubel F and Bill H 1999 *J. Therm. Anal. Cal.* **57** 193–202
[16] Rulmont A 1974 *Spectrochim. Acta* A **30** 161
[17] Jaaniso R, Hagemann H, Kubel F and Bill H 1992 *Chimia* **46** 133
[18] Hagemann H 2006 unpublished results
[19] Rydberg H, Dion M, Jacobson N, Schröder E, Hyldgaard P, Simak S I, Langreth D C and Lundqvist B I 2003 *Phys. Rev. Lett.* **91** 126402
[20] El haj Hassan F, Akbarzadeh H, Hashemifar S J and Mokhtari A 2004 *J. Phys. Chem. Solids* **65** 1871
[21] Mérawa M, Noël Y, Civalleri B, Brown R and Dovesi R 2005 *J. Phys.: Condens. Matter* **17** 535
[22] Sieskind M, Boulou J C, Fettouhi A and Ayachour D 2000 *Mater. Res. Bull.* **35** 1897
[23] Nicollin D and Bill H 1978 *J. Phys. C: Solid State Phys.* **11** 4803